Characteristics of Acoustic Standing Waves in Packed-Bed Columns

T. Sai Kumar, Munesh Kumar Patle, and R. I. Sujith
Indian Institute of Technology, Madras, Chennai-600036, India

DOI 10.1002/aic.11067
Published online December 28, 2006 in Wiley InterScience (www.interscience.wiley.com).

The acoustic characteristics of a column are described when filled with different random packings of various shapes, sizes and void fractions. An experimental setup was developed to study the acoustic field in a packed-bed column. Eight different packings were used to fill the column, and for each packing the acoustic pressure amplitude and phase were measured along the length of the packed bed. The speed of sound and the attenuation coefficient were determined using a nonlinear regression technique. The speed of sound inside the column decreased when the column was filled with packings. The natural frequencies increased as the void fraction of a particular packing decreased. It is shown that the attenuation coefficient depends on a nondimensional frequency defined as $\omega d^2/v$*, where* v *is the kinematic viscosity,* ω *is the angular frequency, and* d *is the effective diameter of the packing.* © 2006 American Institute of Chemical Engineers *AIChE J,* 53: 297–304, 2007

Introduction

Packed towers are vertical columns used for continuous contact of liquid and gases, which have been filled with packing or devices having large surface area to volume ratio. Random packings are simply dumped into the tower during installation and allowed to fall at random. In the past readily available materials, such as broken stone, gravel, or lumps of coke were used. Although inexpensive, they are not desirable for reasons of small surface and poor fluid-flow characteristics. The random packings most frequently used at present are easily obtainable from the chemical industry—the common ones presently manufactured are: Raschig rings, Lessing rings, Partition rings and Pall rings. The liquid once distributed over, trickles down through the packed bed, exposing a large surface to contact the gas. A packed-bed tower is used in the chemical industry to increase the mass-transfer rates by increasing the surface area of exposure between the liquid and gas.

Enhancing the mass-transfer rates of many industrial processes is very critical since this would not only increase the efficiency of these processes, but would also represent huge cuts in the expenditures. The use of acoustic oscillations to enhance heat and mass transfer has been receiving increasing attention in the recent past (Al-Taweel and Landau, 1976; Sujith et al., 2000). Theoretical (Sujith and Zinn, 2000) and experimental (Scarborough et al., 2005) studies have shown that the performance of packed-bed driers can be enhanced under certain conditions, when excited by acoustic oscillations. It has also been shown that the acoustic velocity rather than the acoustic pressure primarily contributes to the mass-transfer enhancement (Scarborough et al., 2005). Hence, it is important to understand the structure of the acoustic field that can be excited in packed-bed towers.

Numerous models were developed to describe the acoustic characteristics of air-filled granular materials (Attenborough et al., 2000, Chotiros et al., 1999). Umnova et al. (2002) developed a model that described the acoustical properties of packings of spheres. Sound propagation in air saturated packings was described by Allard et al. (1998). Buckingham (1997) described the theory of acoustic attenuation, dispersion, and pulse propagation in unconsolidated granular materials. Herrera et al. (2002) developed a model for the sound-pressure distribution inside fluidized beds. The model also computed the speed of sound for fluidized beds, based on the standing-wave theory.

However, no results have been reported on the effect of packing size, packing geometry or sound frequency on the

Correspondence concerning this article should be addressed to R. I. Sujith at sujith@iitm.ac.in

sound-wave patterns in a packed bed. This proved to be the main motivation behind the present investigation on the acoustic characteristics of a packed bed filled with random packings.

Theoretical Background

The packed bed is assumed to behave as a porous medium that resists fluid motion and effects changes in the gas-dynamic properties of the fluid. This assumption is valid for small amplitude acoustic oscillations (operated in the linear regime with a maximum value of p'/p_0 of 0.5%) that are unlikely to affect the packing in the bed. The packed column may be thought of as consisting of a solid material with pores that are interconnected in a random, but isotropic manner. The fluid can percolate through these pores in any direction. The fraction of the volume that is not occupied by the solid is called void fraction and denoted by ε. The solid is assumed to be perfectly rigid and incompressible.

The actual velocity of the fluid as it passes through the "pores" will not be constant in direction or magnitude. However, for the one-dimensional (1-D) model developed here, a mean velocity **u** (x, t) can be defined as the volumetric flow rate per unit cross-sectional area in the bed in a direction along the bed axis. Consequently, at the interfaces of the bed and the gaseous media upstream and downstream of the bed, the mean velocity **u** will be continuous.

The linearized-acoustic continuity and momentum equations for a porous medium can be written as (Morse and Ingard, 1968; Crighton et al., 1992)

$$\frac{\varepsilon}{\rho_0 c_0^2}\frac{\partial p'}{\partial t}+\frac{\partial u'}{\partial x}=0 \tag{1}$$

$$\rho_p\frac{\partial u'}{\partial t}+\phi u'+\frac{\partial p'}{\partial x}=0 \tag{2}$$

Some packings may tend to move with the fluid, thus, adding to its effective mass. Therefore, to express the inertial properties of the fluid in the pores, we use an effective density ρ_p greater than ρ, the density of the fluid in the open. Assuming that the solution has a periodic-time dependence, that is, $p'(x,t) = P'(x)\ e^{i\omega t}$ and $u'(x,t) = U'(x)e^{i\omega t}$, the following equation is derived for the acoustic pressure after eliminating the acoustic velocity

$$\frac{\partial^2 P'}{\partial x^2}+\frac{\omega^2}{c_p^2}\left[1+\frac{\phi}{i\omega\rho_p}\right]P'=0 \tag{3}$$

where $c_p^2 = c_0^2\frac{\rho_p}{\rho_0}\varepsilon$. The wave velocity c_w will then be equal to $c_p\ (1 + \phi/i\rho_p\omega)^{-1/2}$

The above equation is of the form

$$\frac{\partial^2 P'}{\partial x^2}+k'^2P'=0 \tag{4}$$

where $k' = \frac{\omega^2}{c_p^2}[1+\frac{\phi}{i\omega\rho_p}]^{1/2}$ is a modified complex wave number. It must be noted that at low-frequencies, the near presence of the solid material would tend to hold the temperature constant (Morse and Ingard, 1968; Allard, 1998), and c_p would tend towards the isothermal speed of sound, which is lower than the adiabatic speed of sound by a factor of $\gamma^{1/2}$, where γ is the ratio of the specific heats. At very high-frequencies, c_p would tend towards the adiabatic speed of sound. However, it is not established at what frequency the change over takes place.

From Eq. 4 it is seen that by separating the real (k_{real}) and imaginary (k_{imag}) parts of the complex wave number there exists a positive imaginary part, indicating the presence of damping/attenuation in the acoustic field due to the presence of packings. Therefore, for modeling the acoustic field, it is important to determine the damping/attenuation coefficient. In this study, the attenuation factor is determined as a function of various physical parameters to compare the influence of various random packings on the acoustic field of a packed-bed tower. The influence of the packings on the speed of sound of the vibrating air column in the packed-bed column is also important. The natural frequencies of the packed bed are a function of the wave number (k), and the speed of sound (c). Hence, the influence of the packings on the natural frequency of the column is of considerable interest as well.

Experimental Setup and Measurement Technique

The experimental setup consisted of a packed bed—a 1.9 meter column filled with random packings, two acoustic drivers, PCB high-sensitivity piezoelectric transducers (model 106B30, and sensitivity 525mV/psi), a function generator, power amplifiers, data acquisition system, and a cathode ray oscilloscope. The setup is shown in Figure 1. The packed-bed column consisted of a 1.9 meter PVC pipe with dimensions of 110 mm (outer diameter), and a thickness of 8 mm. The column was filled each time with different-random packings of various sizes and shape. The pipe was open at one end while the other end was closed by an aluminum plate of thickness 20 mm. For acoustic pressure measurements, 26 ports (in line) were drilled along the length of the pipe to mount transducers. The first port was at the closed end while the remaining 25 ports were equally spaced at a distance of 7 cm, with the second port at a distance of 12 cm from the

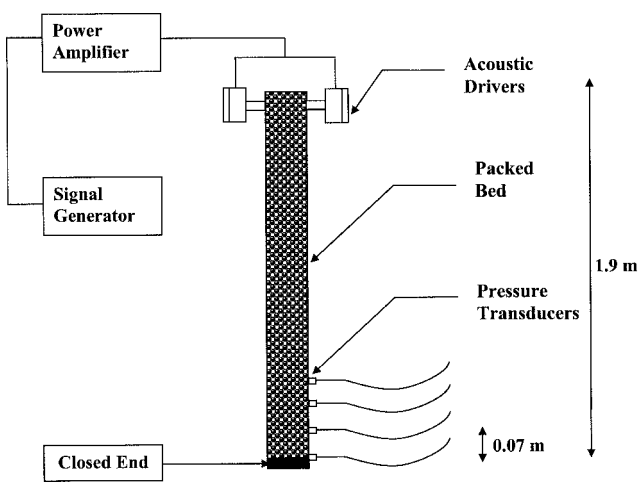

Figure 1. Experimental setup.

closed end. The pressure transducers were placed in these ports in an airtight manner, thus, ensuring that the ports had negligible effect on the sound propagation in the column. Two types of random packings, Raschig rings and Lessing rings were used in the experiments. These packings (cylindrical in shape) were chosen mainly because apart from meeting the experimental requirements they were also readily available off the shelf. The size (outer diameter) of the packings varied from 12 mm to 25 mm, with the void fraction being lowest for the packing having the smallest diameter, and an increase in the diameter of the packing corresponded to an increase in the void fraction of the packings. The experiments were performed at 27°C and at atmospheric pressure.

A pair of acoustic drivers (16-ohm impedance and 100 Watts output) were used to excite standing waves of chosen amplitude and frequency in the column. The frequencies chosen are the natural frequencies of the packed bed, since, at these frequencies maximum sound-pressure level can be obtained with minimum source amplitude. The acoustic drivers were mounted at the open end of the column, and were connected such that they behaved as coherent sources. The natural frequencies were measured experimentally. The acoustic pressure amplitude at the closed end of the packed bed (which is a pressure maximum) was measured for various excitation frequencies. The maximum amplitude was obtained at the resonant frequencies.

The experiment was performed at three natural frequencies of excitation corresponding to the fifth, sixth and seventh modes for each type of packings. These modes were particularly chosen because of the limitations caused by the driver units and the amplifiers; nevertheless similar trends are expected at other modes too. The data obtained for the three modes were analyzed, the acoustic characteristics plotted and the attenuation coefficient was obtained for each of the above cases. The column was then filled with a different packing, and the earlier processes were repeated. Four sizes of packings for each of the Raschig rings type and Lessing rings type were used to fill the column and the characteristics were obtained. The Raschig rings packings that were used had void fractions of 0.9156, 0.8903, 0.8312 and 0.8075, while the Lessing rings packings had void fractions of 0.9008, 0.8666, 0.8011 and 0.7222.

Data Reduction

The steady-state acoustic pressure present at any position along the pipe is given by the expression (Kinsler and Frey, 1962)

$$p' = 2P_0\left(e^{-\alpha x}e^{i[\omega t - kx]} + e^{\alpha x}e^{i[\omega t - kx]}\right) \tag{5}$$

with boundary condition as at $x = 0$, $|p'| = 2P_0$.

Here, α is the attenuation coefficient, k is the wave number, P_0 a constant and $x = 0$ represents a closed end. The real (k_{real}) and imaginary (k_{imag}) parts of the complex wave number k' in Eq. 4 correspond to k (real-wave number) *and*—α (the attenuation coefficient) in Eq. 5. The resulting pressure amplitude at any position along the pipe is given by

$$|P| = 2P_0(\cosh^2 \alpha x \cos^2 kx + \sinh^2 \alpha x \sin^2 kx)^{\frac{1}{2}} \tag{6}$$

The corresponding phase is given by

$$\varphi = \tan^{-1}[\tanh \alpha x \tan kx] \tag{7}$$

Since the transducers were spaced at a distance of 7 cm apart, the exact location of the minima may have not been captured. Hence, to avoid such errors a nonlinear regression technique was used to find the exact location of the minima using the experimental data (Janardhan et al., 1976; Salikuddin and Zinn, 1980). The acoustic pressure was obtained at 26 locations along the packed bed. Denoting $|P_{exp}|$ as the amplitude at each of these locations the acoustic characteristics are obtained in the following manner:

Defining an error function of the form

$$E = \sum_{n=1}^{26}[|P_{th}| - |P_{\exp}|]^2 \tag{8}$$

Substituting for $|P_{th}|$, the theoretically calculated value from Eq. 6 in the earlier expression we get an equation for E in α and k. Minimizing E with respect to α and k yields $\partial E/\partial \alpha = 0$ and $\partial E/\partial k = 0$, resulting in two simultaneous equations (in α and k) which can be solved numerically to obtain α and k.

A sample plot of the experimentally measured acoustic-pressure amplitude and phase, and the corresponding distributions from the regression technique are shown in Figure 2a and 2b respectively for the fifth mode of excitation of the Raschig rings with void fraction 0.8075. From Eq. 6 we see that the nodal points of minimum are given by (Kinsler and Frey, 1962)

$$-kx = \frac{2n-1}{2}\pi \qquad n = 1, 2, 3, \ldots \tag{9}$$

and the amplitudes are given by

$$P_{\min} = 2P_0(\sinh \alpha x) \approx 2P_0(\alpha x) \tag{10}$$

From Eq. 10 we observe that the amplitudes at the minima increase with the corresponding increase in distance from the closed end. This feature is also observed experimentally as can be seen in Figure 2a. Further, it can easily be shown that the amplitudes at the pressure antinodes can be expressed as

$$P_{\max} = 2P_0(\cosh \alpha x) \approx 2P_0(1 + \alpha^2 x^2)^{\frac{1}{2}} \tag{11}$$

This behavior is also seen in these plots. The acoustic waves decay as they travel away from the driver towards the rigid termination. This results in the acoustic amplitudes being higher towards the acoustic driver.

The efficacy of the nonlinear regression technique is well illustrated in the Figures 2a and 2b. In order to estimate the uncertainty in the calculated α and k, a statistical analysis was performed. The acoustic pressure measured by the transducers had an uncertainty of 2%. The experiments were conducted at constant temperature, pressure and humidity to reduce the effect of temperature gradients and other environmental effects. The frequency measurements had an uncertainty of 0.1%, and was verified by transducer measurements. These uncertainties were specified by the manufacturer for the respective hardware. The uncertainty involved in the

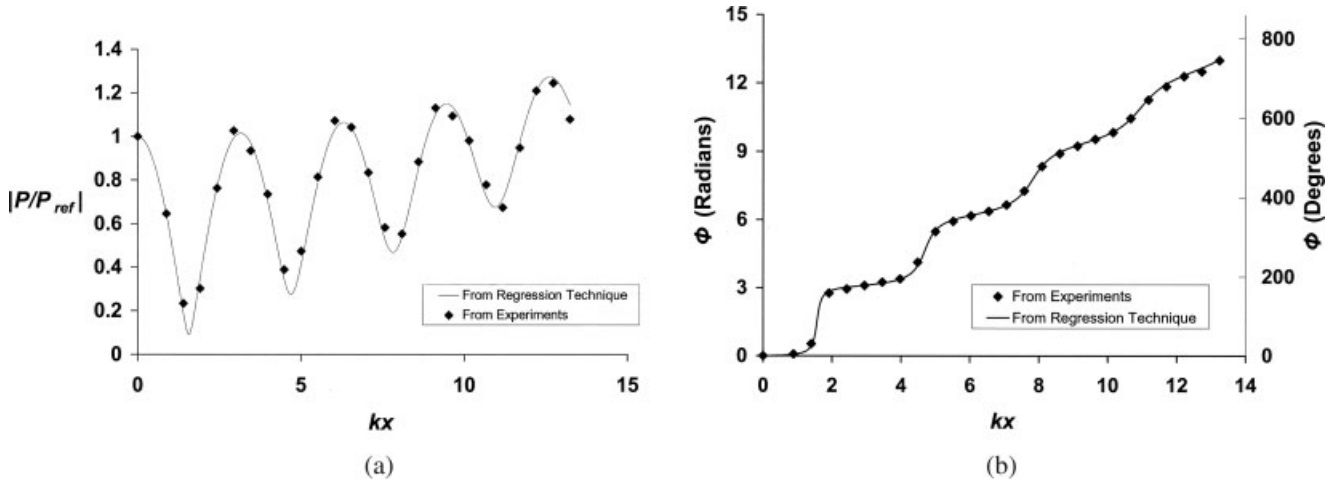

Figure 2. (a) Sample plot showing the comparison between the experimentally determined acoustic pressure amplitude distribution (normalized with the closed end amplitude), and the acoustic pressure amplitude obtained from the non-linear regression analysis for the 5th mode of the Raschig ring having void fraction ε = 0.8075 (calculated values of α and k are 0.425 m^{-1} and 7.3577 m^{-1}, respectively); (b) sample plot showing the comparison between the experimentally determined acoustic phase difference distribution (with respect to the closed end), and the acoustic phase difference obtained from the nonlinear regression analysis for the 5th mode of the Raschig ring, having void fraction ε = 0.8075 (calculated values of α and k are 0.425 m^{-1} and 7.3577 m^{-1}, respectively).

(a) Correlation coefficient = 0.9846; (b) Correlation coefficient = 0.9980.

measurement of the void fraction of the packings was 0.2%. The uncertainty in the acoustic pressure was taken into consideration, while determining the errors involved in the nonlinear regression technique, and the error analysis showed that the attenuation constant, and the wave number had an uncertainty of 0.5% each. Also the speed of sound calculated using the values of the attenuation constant and wave number had an uncertainty of 1.5%. The errors in the earlier calculations were found using the standard error analysis technique of finding the individual relative errors associated with each of the variables, and then defining the overall error propagation to be the sum of the relative errors (Taylor, 1982).

The size of the packings was much smaller than the diameter of the duct; hence, the results are not biased by the

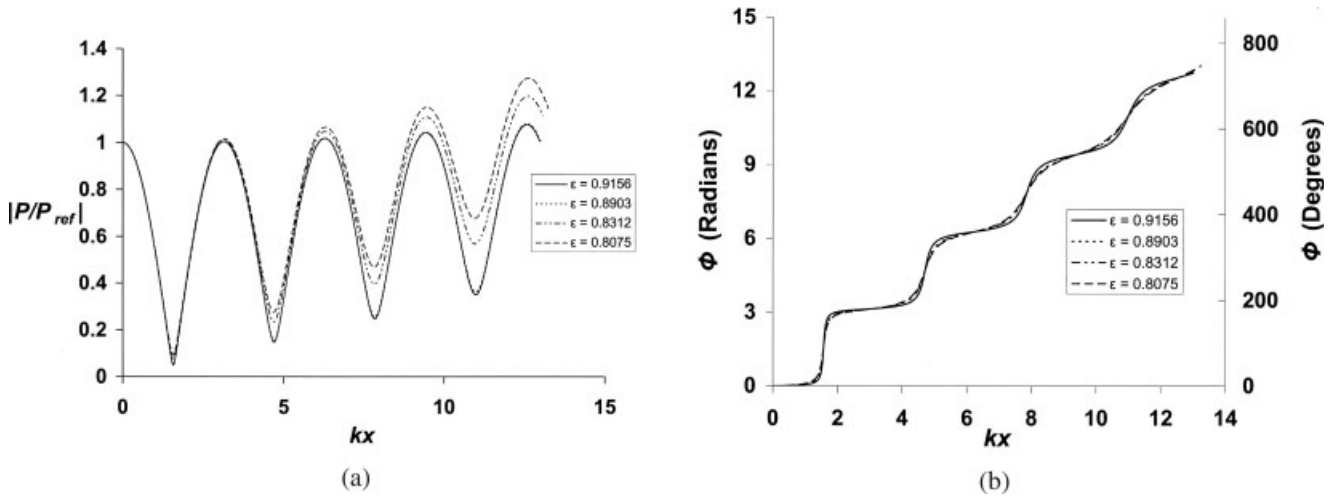

Figure 3. (a) Variation in acoustic pressure amplitude (normalized with the closed end amplitude) with axial distance for the fifth mode of acoustic excitation for the Raschig rings type packings, having void fractions of 0.9156, 0.8903, 0.8312 and 0.8075, at frequencies of 304 Hz, 294 Hz, 290 Hz and 284 Hz, respectively; (b) variation in acoustic phase (with respect to the closed end) with axial distance for the fifth mode of acoustic excitation for the Raschig rings type packings, having void fractions of 0.9156, 0.8903, 0.8312 and 0.8075, at frequencies of 304 Hz, 294 Hz, 290 Hz and 284 Hz, respectively.

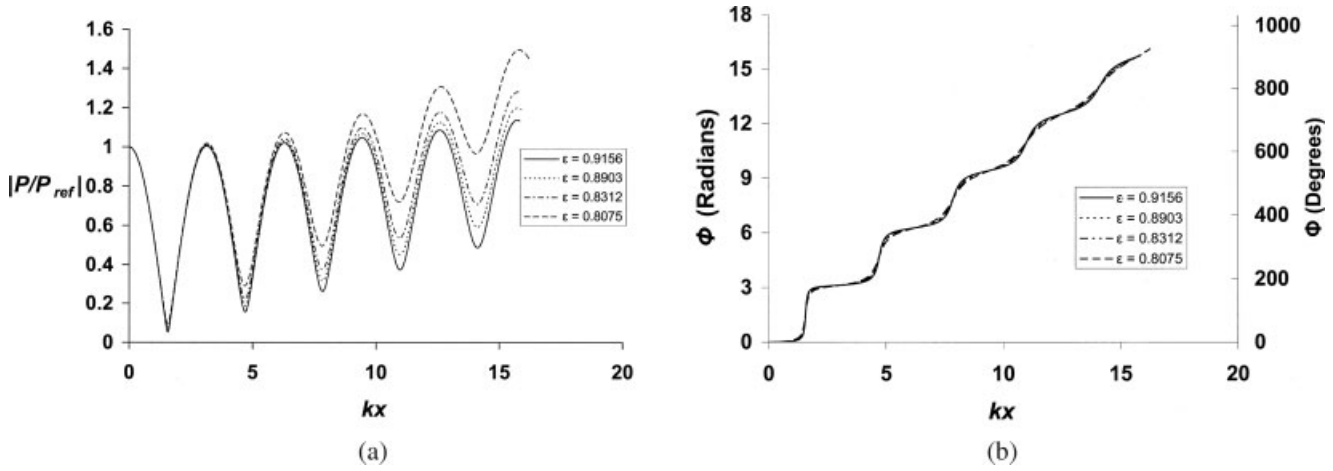

Figure 4. (a) Variation in acoustic pressure amplitude (normalized with the closed end amplitude) with axial distance for the sixth mode of acoustic excitation for the Raschig rings type packings, having void fractions of 0.9156, 0.8903, 0.8312 and 0.8075, at frequencies of 373 Hz, 361 Hz, 355 Hz and 351 Hz, respectively; (b) variation in acoustic phase (with respect to the closed end) with axial distance for the sixth mode of acoustic excitation for the Raschig rings type packings, having void fractions of 0.9156, 0.8903, 0.8312 and 0.8075, at frequencies of 373 Hz, 361 Hz, 355 Hz and 351 Hz, respectively.

random orientation of the packings. A statistical approach was used to ascertain this, by repeating the experiments (with the column being filled with the same packings) a few times. The results obtained were well within the uncertainty limits stated in the article.

Experimental Results

The acoustic pressure amplitude and phase variation along the nondimensional-axial distance (kx) for the standing wave in the packed-bed column for Raschig rings are shown in Figures 3–5. In these plots, the acoustic-pressure amplitude is normalized with the pressure amplitude at the closed end (P_{ref}) and $x = 0$ on the horizontal axis represents the closed end. There was no dependence of the acoustic-pressure distribution on the pressure amplitude at the closed end which was varied from 30 Pascals to 300 Pascals, indicating that the sound propagation is essentially linear. The linear attenuation is mainly because of the viscous and thermal-boundary layer effects in the column. At higher-pressure amplitudes, the nonlinear propagation would lead to the generation of harmonics, leading to a distortion of the wave. At amplitudes that are high enough, shockwaves may be formed (Naugolnykh and Ostrovsky, 1998). In the phase angle plots, the phase angle is calculated with respect to the closed end, and $x = 0$ represents the closed end on the horizontal axis. All phase angles are in radians.

Figures 3a, 4a and 5a show the variation in the acoustic-pressure amplitude, as a function of the nondimensional-axial

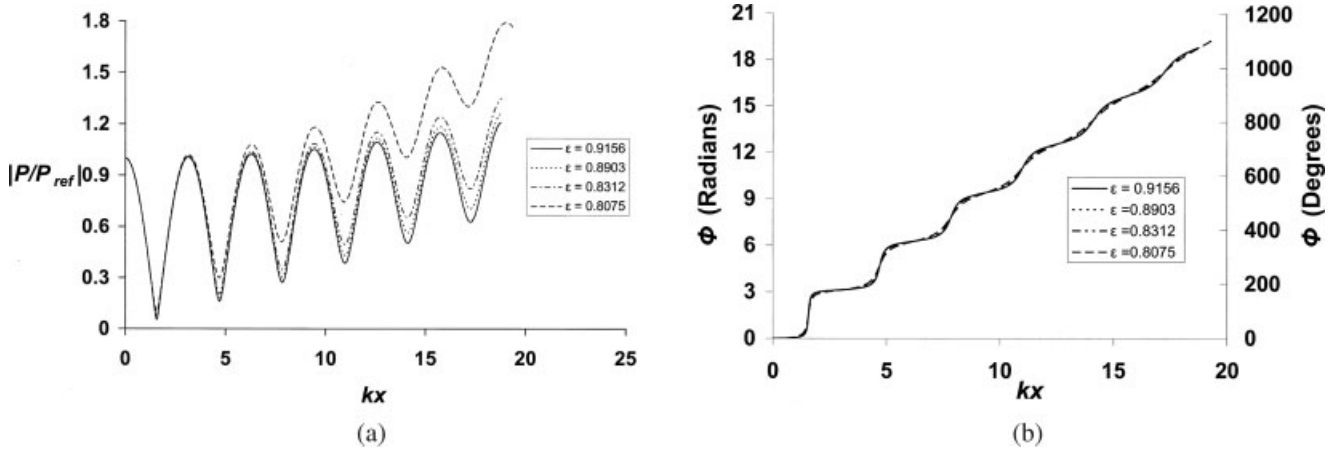

Figure 5. (a) Variation in acoustic pressure amplitude (normalized with the closed end amplitude) with axial distance for the seventh mode of acoustic excitation for the Raschig rings type packings, having void fractions of 0.9156, 0.8903, 0.8312 and 0.8075, at frequencies of 422 Hz, 428 Hz, 420 Hz and 418 Hz, respectively; (b) variation in acoustic phase (with respect to the closed end) with axial distance for the seventh mode of acoustic excitation for the Raschig rings type packings, having void fractions of 0.9156, 0.8903, 0.8312 and 0.8075, at frequencies of 422 Hz, 428 Hz, 420 Hz and 418 Hz, respectively.

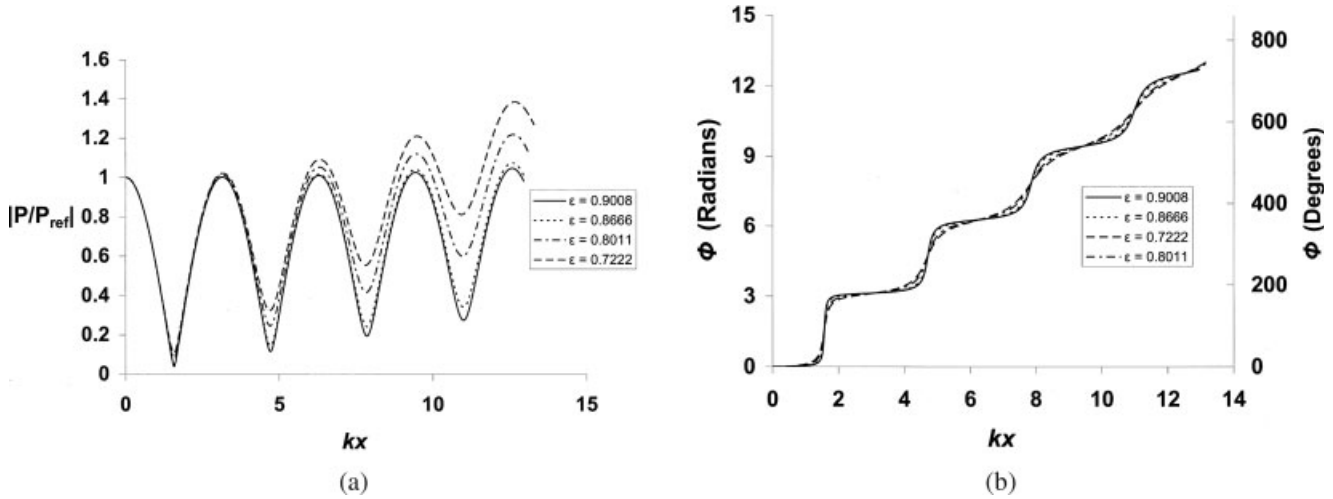

Figure 6. (a) Variation in acoustic pressure amplitude (normalized with the closed end amplitude) with axial distance for the fifth mode of acoustic excitation for the Lessing rings type packings, having void fractions of 0.9008, 0.8666, 0.8011 and 0.7222, at frequencies of 306 Hz, 299 Hz, 290 Hz and 286 Hz, respectively; (b) variation in acoustic phase (with respect to the closed end) with axial distance for the fifth mode of acoustic excitation for the the Lessing rings type packings, having void fractions of 0.9008, 0.8666, 0.8011 and 0.7222, at frequencies of 306 Hz, 299 Hz, 290 Hz and 286 Hz, respectively.

distance (kx), along the length of the column when excited in the fifth, sixth and seventh modes for the four types of Raschig-ring packings. The pressure amplitude at the node keeps increasing as we move away from the closed end (at $x = 0$). This increase is higher for higher frequencies and lower-void fractions. The variation in phase angle (Figures 3b, 4b, 5b) becomes more gradual at higher-frequencies and lower-void fractions. These trends are indicative of the acoustic attenuation. Figures 6a and 6b show similar trends in the case of Lessing Rings—in the interest of space the plots are shown for one void fraction only.

Attenuation coefficient

From the graphs of the variation in acoustic pressure amplitude with the axial distance (kx) it is observed that, for a given random packing (shape), the acoustic attenuation increases with decrease in void fraction. The attenuation is higher at higher-frequencies. Furthermore, the attenuation coefficient is seen to vary with the type of packing used to fill the column. From the measurement of the acoustic-standing wave, the attenuation coefficient was quantified using the data-reduction procedure described earlier. The variation in attenuation coefficient as a function of the void fraction for various modes (frequencies) is shown in Figures 7a and 7b for Raschig rings and Lessing rings, respectively. These plots show similar trends for both the types of packings.

In summary, the attenuation coefficient depends on the excitation frequency ω, the effective diameter of the packing d ($d = 6(1 - \varepsilon)/a_p$ is the diameter of a sphere having the same surface to volume ratio as the packing, where a_p is the specific area), the kinematic viscosity v (since the attenuation

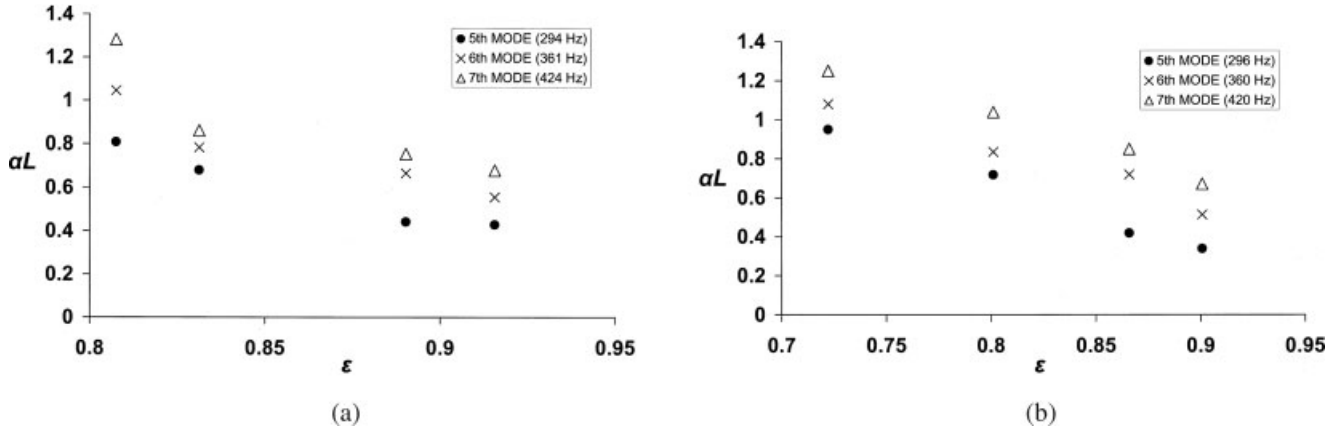

Figure 7. (a) Variation in attenuation coefficient (nondimensionalized) with the void fraction for the four Raschig rings type packings when excited at 3 different acoustic modes; (b) variation in attenuation coefficient (nondimensionalized) with the void fraction for the four Lessing rings type packings when excited at three different acoustic modes.

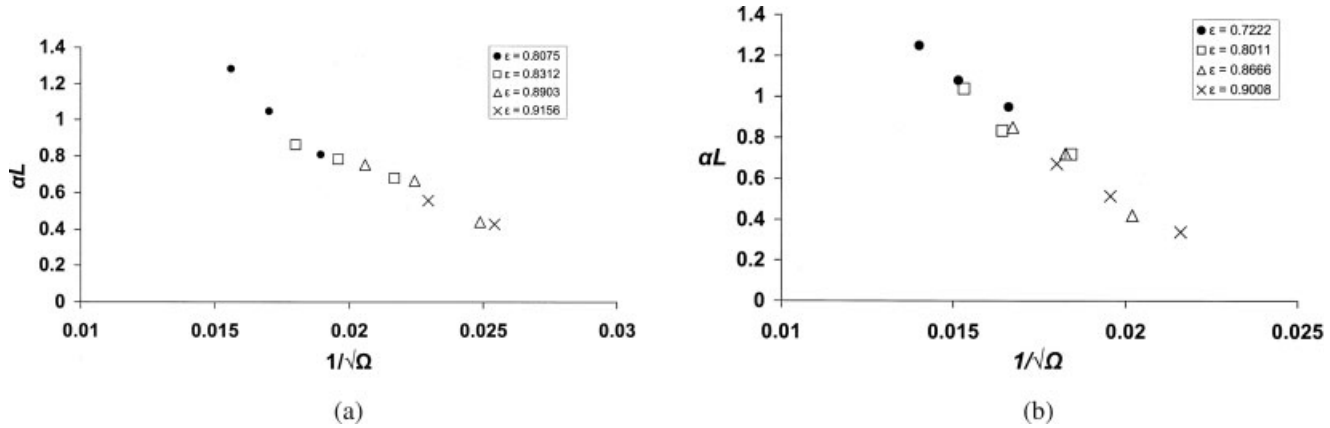

Figure 8. (a) Variation of the attenuation coefficient (nondimensionalized) with nondimensional frequency for the four Raschig rings type packings; (b) variation of the attenuation coefficient (nondimensionalized) with nondimensional frequency for the four Lessing rings type packings.

will depend on the frictional resistance), and the type of packing present in the column; that is $\alpha = f(\omega, d, \nu,$ type of packing)

Using dimensional analysis it can be shown that

$$\alpha = f\left(\frac{\omega d^2}{\nu},\ \text{type of packing}\right) \tag{12}$$

where, $\omega d^2/\nu$ can be interpreted as a nondimensional frequency, denoted by Ω.

Figures 8a and 8b show the variation of the nondimensional-attenuation coefficient (αL), as a function of the nondimensional frequency. It can be seen that the curves in Figures 8a and 8b, indeed collapse into one.

The physical significance of the nondimensional frequency can be seen by recasting it as follows

$$\Omega = \frac{\omega d^2}{\nu} = \frac{Ud}{\nu}\frac{\omega d}{U} = Re\ St \tag{13}$$

where Re is the Reynolds number, and St is the Strouhal number. The attenuation coefficient depends on the drag, and, hence, is a function of Reynolds number. Furthermore, it should also be a function of the ratio of the flow, and acoustic time scales, which is expressed by the Strouhal number.

$$St = \frac{\omega d}{U} = 2\pi\frac{d/U}{\lambda/c}, \tag{14}$$

where λ is the wavelength and c is the speed of sound.

Speed of sound

The values of α ($-k_{imag}$) and k (k_{real}) obtained were used to determine the speed of sound from the equation

$$k_{real}^2 - k_{imag}^2 = \omega^2/c_p^2 \tag{15}$$

obtained by separating the real and imaginary parts of the complex-wave number (Eq. 4). The phase velocity c_w is roughly equal to c_p, when $\omega \gg \phi/\rho_p$ as is the case here. Figure 9 shows the variation of c_p as a function of the void fraction of the packings. From Figure 9, it is observed that the speed of sound is lower for the packings having low-void fractions than for packings with high-void fractions. The speed of sound did not show frequency dependence in the range of frequencies studied here, within the experimental uncertainty. It is further observed that the speed of sound of the vibrating air column is lower for the Raschig rings than for the Lessing Rings. Also, the number of modes in the same frequency range is higher when the pipe was filled with packings than for the case of the empty pipe. Once the speed of sound decreases, the natural frequency for the same mode also decreases. The trends observed (experimentally) in the change in natural frequencies for the Raschig rings and the Lessing rings type packing is shown in Table1.

The speed of sound is proportional to the square root of the ratio of the stiffness to the mass. The stiffness is increased by the removal of air in the column due to the packings. At low-frequencies, the near presence of the solid material would tend to hold the temperature constant (Morse and Ingard, 1968; Allard, 1998), and it would tend toward the isothermal stiffness, which is lower than the adiabatic stiffness by a factor of γ, the ratio of the specific heats. Furthermore, some of the packings may move with the fluid, thus, adding to its effective mass. At low-frequencies, the decrease in speed of sound can be explained in terms of the contribution from these factors. A lower bound for speed of

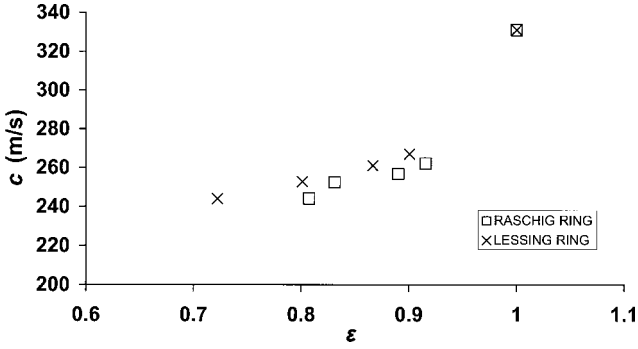

Figure 9. Change in speed of sound of the air column in the packed bed when filled with each of the two kinds of packings.

Table 1. Variation in Natural Frequencies with Void Fractions for the Raschig Rings and Lessing Rings Type Packings

Type of Packing	Packing Size (Outer dia.)	Void Fraction	Natural Frequencies (Hz)		
			5th mode	6th mode	7th mode
Raschig rings	12 mm	0.8075	284	351	418
	15 mm	0.8312	290	355	420
	20 mm	0.8903	294	361	428
	25 mm	0.9156	304	373	422
Lessing rings	12 mm	0.7222	286	344	402
	15 mm	0.8011	290	365	420
	20 mm	0.8666	299	366	436
	25 mm	0.9008	306	373	440
Empty duct	–	1	394	481	568

sound will then be $\frac{\bar{P}\rho_p\varepsilon}{\rho_0^2} = c^2_{\text{isothermal}}\frac{\rho_p}{\rho_0}\varepsilon$. At high-frequencies, one can think that the sound waves must travel a longer distance due to the tortuous path that must be followed as the waves are scattered through the pores in the packed bed.

Conclusions

The acoustic characteristics of a packed-bed column were investigated. The acoustic attenuation increased with increase in frequency and decrease in void fraction. The attenuation coefficient was shown to be a function of $v/\omega d^2$ (v is the kinematic viscosity, ω is the angular frequency, and d is the effective diameter of the packing) and the type of packing. The speed of sound decreased with decrease in void fraction. The natural frequencies were found to increase with decreasing void fraction.

Acknowledgments

This research was funded by a grant from the Ministry of Human Resource and Development of India (MHRDI).

Notation

a_p = specific area of packings
c_0 = speed of sound in air, m/s
c_p = speed of sound in the packed bed column, m/s
c_w = wave velocity, m/s
D = mean-particle diameter
K = wave number
K' = complex-wave number
p' = acoustic pressure
$\bar{P}$ = mean pressure
P_{exp} = experimental pressure amplitude
P_{th} = theoretical pressure amplitude
P_0 = constant of Integration
$Phase$ = phase difference (with respect to the closed end)
$\Omega = \frac{1}{d}\sqrt{\frac{v}{\omega}}$
$P'(x)$ = acoustic pressure variation in space
U' = acoustic velocity
$U'(x)$ = acoustic velocity variation in space

Greek Letters

α = non dimensionalised attenuation coefficient
E = void fraction of packings
P = density of air
ρP = effective density of air
Φ = frictional resistance
Λ = ratio of specific heats
Y = kinematic viscosity of air
Ω = angular frequency
Ω = nondimensional frequency

Literature Cited

Allard, J. F., M. Henry, J. Tizianel, L. Kelders, and W. Lauriks, "Sound Propagation in Air-Saturated Random Packings of Beads," *J. Acoust. Soc. Am.*, **104**(4), 2004–2007 (1998).

Al-Taweel, A. M., and J. Landau, "Mass Transfer between Solid Spheres and Oscillating Fluids - A Critical Review," *The Canadian J. of Chem. Eng.*, **54**, 532–539 (1976).

Attenborough, K., O. Umnova, and K. M. Li, "Cell Model Calculations of Dynamic Drag Parameters in Packings of Spheres," *J. Acoust. Soc. Am.,* **107**(6) 3113–3119 (2000).

Buckingham, M. J., "Theory of Acoustic Attenuation, Dispersion, and Pulse Propagation in Unconsolidated Granular Materials including Marine Sediments," *J. Acoust. Soc. Am.*, **102**(5), Pt. 1, 2579–2596 (1997).

Chotiros, N. P., D. J. Yelton, and M. Stern, "An Acoustic Model of Laminar Sand Bed," *J. Acoust. Soc. Am.,* **106**(4), Pt. 1 1681–1693 (1999).

Crighton, D. E., A. P. Dowling, J. E. Ffowcs Williams, M. Heckl, and F. G. Leppington, Modern Methods in Analytical Acoustics, New York: Springer, N. Y. (1992).

Herrera, O. A., and E. K. Levy, "Characteristics of Acoustic Standing Waves in Fluidized Beds," *AIChE*, **48**(3), 503–644 (2002).

Janardhan, B. A., B. R. Daniel, and B. T. Zinn, "Measurements of Acoustic Responses of Gaseous Propellant Injectors," *J of Sound and Vibration*, **47**(4): 559–569 (1976).

Lafarge, D., P. Lemarinier, J. F. Allard, and V. Tarnow, "Dynamic Compressibility of Air in Porous Structures at Audible Frequencies," *J. of Acoust. Soc. of Am.*, **102**, 1995–2006 (1997).

Kinsler, L. E., and A. R. Frey, Fundamental of Acoustics, Wiley New York. (1962).

Morse, P. M., and K. U. Ingard, Theoretical Acoustics, New York, McGraw-Hill (1965).

Taylor, J. R., *An Introduction to Error Analysis: The Study of Uncertainties in Physical Measurements*, Oxford University Press, University Science Books (1982).

Naugolnykh, K., and L. Ostrovsky, *Nonlinear Wave Processes in Acoustics*, *Cambridge Texts in Applied Mathematics* (1998).

Salikuddin, M., and B. T. Zinn, "Adaptation of the impedance tube technique for the measurement of combustion process admittances," *J. of Sound and Vibration,* **68**(1), 119–132 (1980).

Scarborough, E. D., R. I. Sujith, and B. T. Zinn, "The Effect of Resonant Acoustic Oscillations on Heat and Mass Transfer rates in a Convection Air Dryer," *J. of Drying Technol.*, **24**(8), 931 (2006).

Sujith, R. I. and B. T. Zinn, "A Theoretical Investigation of Enhancement of Mass Transfer from a Packed Bed using Acoustic Oscillation," *Canad. J. of Chem. Eng.*, **78**, 1145–1150 (2000).

Umnova, O., K. Attenborough, and K. M. Li. "A Cell model for the Acoustical Properties of Packings of spheres," *J. Acoust. Soc. Am,* **87**(6), 226–235 (2001).

Manuscript received Aug. 22, 2005, and revision received May 15, 2006 and final revision received Nov. 10, 2006.